Geophysical evidence for chemical variations in the Australian Continental Mantle

Luuk van Gerven,[1] Frédéric Deschamps,[1] and Robert D. van der Hilst[1,2]

[1] The relative density-to-shear velocity scaling (ζ) provides a diagnostic for the presence of compositional variations in the mantle. We invert shear-wave velocity from a recent 3-D model and gravity anomalies for radial profiles of ζ of the uppermost mantle beneath Australia. We performed calculations for the three major tectonic provinces that constitute the continent, and found significant differences between them. The ζ profile for the Phanerozoic region can be explained by thermal variations alone. In contrast, negative values of ζ suggest that variations in composition are important between ~75 and ~150 km depth in the Proterozoic continental lithosphere (central Australia). It is likely that chemical variations are also required to explain the inferences for the Archean craton (west Australia), but poor tomographic resolution precludes a definitive conclusion. The scaling factors found are consistent with chemical depletion of deep Precambrian lithosphere, which supports a tectosphere model for the Australian continental roots.   INDEX TERMS: 1212 Geodesy and Gravity: Earth's interior—composition and state (8105, 8124); 8124 Tectonophysics: Earth's interior—composition and state (1212); 8120 Tectonophysics: Dynamics of lithosphere and mantle—general; 7218 Seismology: Lithosphere and upper mantle. Citation: van Gerven, L., F. Deschamps, and R. D. van der Hilst (2004), Geophysical evidence for chemical variations in the Australian Continental Mantle, Geophys. Res. Lett., 31, L17607, doi:10.1029/2004GL020307.

1. Introduction

[2] Precambrian cratons are postulated to be underlain by thick continental roots [e.g., *Jordan*, 1978; *Polet and Anderson*, 1995] which stabilized shortly after their formation and have remained coupled to the crust ever since [*Griffin et al.*, 1998]. The nature of these roots and the cause of their long-term stability are still debated [see, e.g., *Shapiro et al.*, 1999a; *Lenardic and Moresi*, 1999]. Ancient continental roots are thought to be colder than oceanic or younger continental lithosphere [*Forte and Perry*, 2000; *Artemieva and Mooney*, 2001] but gravity anomalies and the geoid do not correlate with craton locations [*Jordan*, 1978; *Shapiro et al.*, 1999b]. *Jordan* [1978, 1988] thus postulated that the density increase due to the cooling of the root is balanced by chemical depletion in basaltic components with respect to the average mantle. This iso-pycnic equilibrium is an essential part of the so called "tectosphere" hypothesis,

but the need for compositional differentiation has been questioned [e.g., *Pari and Peltier*, 1996]. In addition, the rheology of the continental lithosphere (CL) could play an important role in its formation and stabilization over geological time [*Jordan*, 1988; *Shapiro et al.*, 1999a; *Lenardic and Moresi*, 1999].

[3] To determine if a tectosphere is present beneath Australia we investigate the ratio of relative changes in density and shear speed (ζ), a diagnostic for variations in composition:

$$\zeta(r, \theta, \varphi) \equiv \frac{\partial \ln \rho(r, \theta, \varphi)}{\partial \ln V_S(r, \theta, \varphi)}. \tag{1}$$

Predominance of thermal effects produces positive values of ζ. The precise effect of changes in bulk chemistry on ζ is not well-defined, but depletion in dense elements (e.g., iron or basaltic components) would decrease the amplitude of density anomalies. Small and negative values of ζ therefore indicate that effects of composition are significant. Global scale investigations have determined depth profiles of ζ for continental and oceanic regions [e.g., *Forte et al.*, 1994; *Deschamps et al.*, 2001], and presented evidence for chemical depletion in the tectosphere [*Forte and Perry*, 2000; *Deschamps et al.*, 2002]. More recently, *Perry et al.* [2003] proposed a detailed regional study for North America.

[4] The SKIPPY seismometry project [*van der Hilst et al.*, 1994] has enabled the construction of detailed wavespeed models of the continental upper mantle beneath Australia [e.g., *Zielhuis and van der Hilst*, 1996; *Debayle and Kennett*, 2000, 2003; *Simons et al.*, 1999, 2002; *Yoshizawa and Kennett*, 2004]. Here we will use an update, hereinafter referred to as *AUS04-Vs*, of the isotropic part of the model by *Simons et al.* [2002]. We use gravity anomalies according to *EGM96* [*Lemoine et al.*, 1998].

[5] The Australian continent can be divided in three main tectonic provinces (Figure 1a) with a westward age progression from Phanerozoic (<500 Ma), to Proterozoic (500–2500 Ma), and Archean (>2500 Ma). If parts of the Australian continent are underlain by a tectosphere one would expect lateral variations in the depth profiles $\zeta(r)$. Indeed, research presented here suggests that depth profiles for these domains differ from one another and that they can be used to constrain the depth range of chemical depletion.

---

[1]Department of Geophysics, Utrecht University, Utrecht, Netherlands.
[2]Now at Department of Earth, Atmospheric, and Planetary Sciences, Massachusetts Institute of Technology, Cambridge, Massachusetts, USA.

2. Methodology

[6] We invert gravity (δg) and shear-wave velocity anomalies (δV_S) for radial changes in the scaling factor
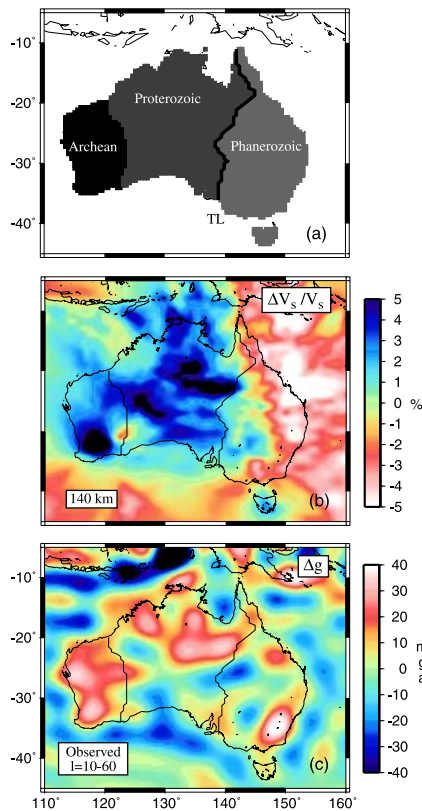
Figure 1. (a) Age-regionalization of the Australia continent. We considered three major regions: Archean, Proterozoic, and Phanerozoic. Across the continent, the age of the crust increases from East to West. *TL* denotes the Tasman Line. (b) Relative shear-velocity anomalies at z = 140 km according to model *AUS04-V$_S$*. The reference model is *ak135*. (c) Observed gravity anomalies derived from *EGM96* and crustal correction according to *CRUST2.0*. Data are filtered for spherical harmonic degrees $\ell = 10 - 60$.

$\zeta(r, \theta, \varphi)$. To model gravity anomalies we integrate density anomalies $\delta\rho$ vertically and laterally following

$$
\delta g(\theta, \varphi) = \frac{3g_0}{4\pi\overline{\rho}R} \int_{r_{CMB}}^{R} \int_{0}^{\pi} \int_{-\pi/2}^{\pi/2} K_g(\Delta, r) \cdot \delta\rho(r, \theta', \varphi')
$$
$$
\cdot \sin\theta' d\theta' d\varphi' dr, \tag{2}
$$

where R and $\overline{\rho}$ are the Earth's radius and mean density, respectively, r_{CMB} the radius of the core-mantle boundary, g_0 the surface acceleration of gravity, $K_g(\Delta, r)$ the local gravity kernels, and Δ the angular distance between the locations (θ, ϕ) and (θ', ϕ'). This equation is similar to that used by *Kogan and McNutt* [1993].

[7] We perform the analysis in the part of the spectral domain that is sensitive to the uppermost mantle. Spherical harmonic degrees lower than $\ell = 10$ sample the whole mantle and are removed to avoid smearing effects. To focus the study on the depth interval $50-300$ km and reduce the influence of the crust we also removed degrees higher than $\ell = 60$. For the band-pass filtering, $\ell_1 \leq \ell \leq \ell_2$, the local gravity kernels are given by

$$
K_g(\Delta, r) = \sum_{\ell=\ell_1}^{\ell_2} (\ell - 1) \cdot G_\ell(r) \cdot P_\ell^0(\cos\Delta), \tag{3}
$$

where $P_\ell^0(\cos \Delta)$ are Legendre polynomials and $G_\ell(r)$ the radial geoid kernels. The latter depend strongly on the radial viscosity profile and boundary topography and are computed using the method proposed by *Forte and Peltier* [1991] and viscosity profile MF2 due to *Mitrovica and Forte* [1997]. Interestingly, geoid kernels for degrees higher than $\ell = 10$ depend only slightly on the viscosity profile. An important consequence is that within error bars, the scaling factor for the uppermost mantle (z < 400 km) is not sensitive to viscosity [*Deschamps et al.*, 2001].

[8] Radial geoid kernels (and therefore local gravity kernels) for degrees $\ell = 10$ to 60 are sensitive to the upper mantle but have negligible values throughout the lower mantle. The depth integration in equation (2) can then be reduced to the layer $35 \leq z \leq 670$ km. For different depths, Figure 2 shows the local gravity kernels for $\ell = 10 - 60$. The amplitude of local gravity kernels decreases rapidly with increasing angular distance. This justifies the use of truncated local kernels, which are equal to the local kernels for angular distances smaller than a cut-off angular distance (Δ_c) and zero elsewhere. Here we present results for $\Delta_c = 12°$.

[9] Substitution of equation (1) into equation (2) gives a linear relation between δg, δV_S, and ζ. We use a generalized inversion to estimate ζ from δg and δV_S. We performed simultaneous inversions for each age-region represented in Figure 1a. The regularization is controlled by a damping factor ε. Increasing ε enhances the smoothness of $\zeta(r)$ but leads to higher misfit of the reconstructed data with respect to the observed data. We inferred the optimal value of ε from the trade-off curves shown in Figure 3 and investigated the sensitivity of the solution to the choice of ε.

[10] The (isotropic) shear-wave velocity model *AUS04-Vs* is defined on a $1° \times 0.5°$ lateral grid and for 10 depth layers [see, e.g., *Zielhuis and Van der Hilst*, 1996]. The lateral resolution is ~300 km in eastern and central Australia but degrades toward the Archean west owing to reduced wave path coverage. Figure 1b shows *AUS04-Vs* at 140 km depth. Figure 1c depicts the tide-free, non-hydrostatic free-air gravity anomalies from *EGM96*, filtered for the spectral window $\ell = 10 - 60$. We assumed that the crust is in hydrostatic equilibrium and we used *CRUST2.0* [*Bassin et al.*, 2000] to remove its contribution to gravity anomalies.

[11] The main sources of uncertainty are the errors in the tomographic and crustal models. In absence of formal estimates of error in wavespeed, we studied the effect of random noise generated from a Gaussian probability distribution with zero mean and a standard deviation (σ_{err}) equal to 50% of the RMS of the *AUS04-Vs* values at the depth considered. For each layer of CRUST2.0, the σ_{err} of the
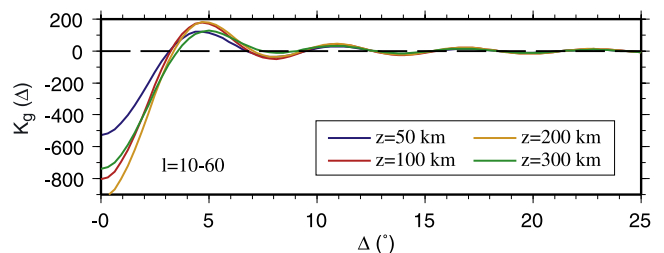

Figure 2. For four different depths, the local gravity kernels (K_g) are shown as a function of angular distance Δ. The spectral window is $\ell = 10 - 60$.
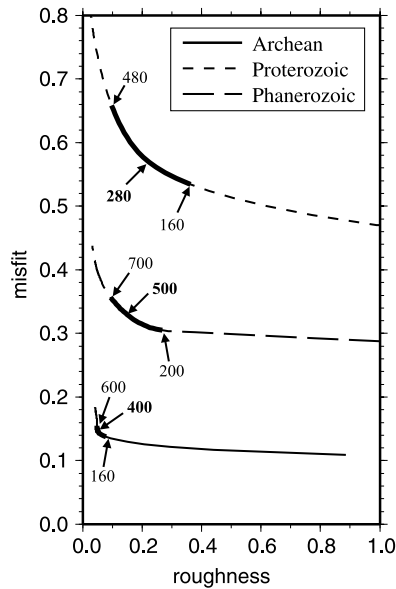
Figure 3. Trade-off between data misfit and model roughness for the three age regions. The bold segments of the trade-off curves indicate the ranges of acceptable values for damping factor ε. The preferred values are indicated in bold. Data filtered for degrees $\ell = 10 - 60$.

error distribution used is 1% of the layer density, but near layer boundaries we use 5% to mitigate effects of incorrect interface depths. We then produced 1000 perturbed V_S and crust models, and we inverted each of them for ζ as a function of depth. At each depth, the mean and standard deviation of the 1000 perturbed profiles thus produced are used as estimates of the scaling factor $ζ(r)$ and its uncertainty, $σ_ζ$.

3. Results

[12] The solid curves in Figures 4a–4c represent the average scaling factor $ζ(r)$ for each region, and the error bars represent one standard deviation uncertainty, $σ_ζ$. Fortunately, even the generous a priori errors described above do not lead to very large uncertainty in ζ. For reference, we depict with grey shading the thickness of the Phanerozoic and Proterozoic CL as estimated from the high wavespeed lid in *AUS04-Vs*; the Archean CL is poorly resolved by the seismic data used [*Simons et al.*, 2002]. The average scaling factor for Phanerozoic is positive throughout the CL (Figure 4a). It is perhaps slightly negative between 130 and 190 km depth, coincident with the seismic low velocity zone [*Zielhuis and van der Hilst*, 1996], but the large error bars may render this insignificant. The scaling factor profile for the Proterozoic is more complicated. Within error, ζ is positive to a depth of 75 km, negative between 75 and 150 km depth, and statistically zero below. Finally, the average scaling factor for Archean is smaller in amplitude than both others and is negative to a depth of ∼200 km (Figure 4c). The negative values appear statistically significant, but we recall that resolution of wavespeed anomalies is poor in this part of the model [e.g., *Simons et al.*, 2002].

[13] It is important to assess the robustness of our results. First, the resolution matrices (Figures 4d–4f) demonstrate

that the scaling factors for the Phanerozoic and Proterozoic are well resolved down to ∼300 km. Below that depth (not shown here) substantial smearing occurs due to decreasing values of the gravity and surface wave sensitivity kernels. The scaling factor for Archean is poorly resolved even for depths less than 300 km. Second, we computed profiles of scaling factors for several values of the damping factor ε. For low values of ε, profiles are less smooth and uncertainties are larger. However, the shapes of the profiles and, in particular, the negative values between 75 and 150 km depth for the Proterozoic, are fairly robust. Finally, to investigate the influence of the spectral window, we performed calculations for $\ell = 10 - 40$, $\ell = 20 - 60$, and $\ell = 10 - 80$, but we did not find significant changes. We thus conclude that the $ζ(r)$ inferred for the Phanerozoic and Proterozoic are robust down to 300 km depth.

4. Discussion and Concluding Remarks

[14] The Phanerozoic CL extends down to at most 120 km depth [e.g., *Zielhuis and van der Hilst*, 1996], and the positive scaling factor across this top layer can be explained
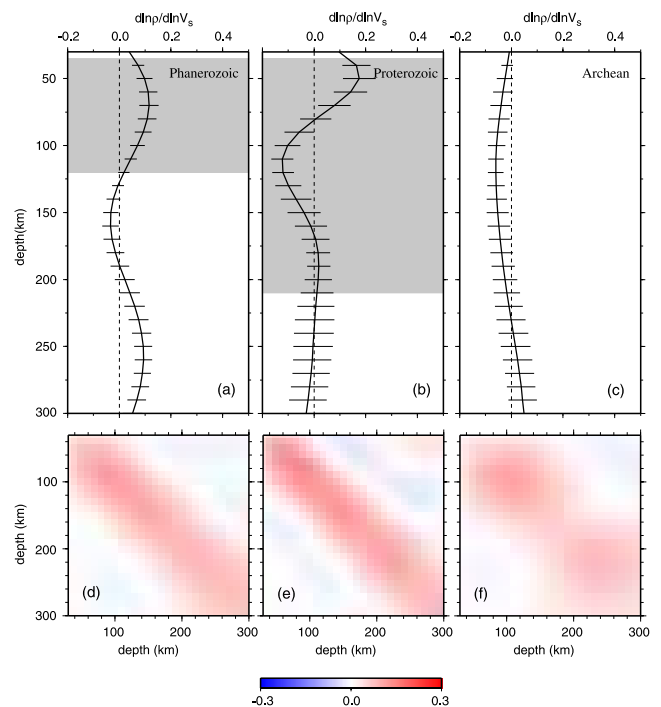

Figure 4. Radial model of scaling factor (equation (1)) for the three age-regions defined in Figure 1a. (a) Phanerozoic; (b) Proterozoic; and (c) Archean. The solid curves represent the average value of ζ at a given depth, and the error bars depict one standard deviation around this average. Error bars are estimated by generating random errors in the tomographic model and the crustal models, assuming Gaussian probability distributions (see text). Data are filtered for degrees $\ell = 10 - 60$, and the damping factor is 400, 280, and 500 for the Archean, Proterozoic, and Phanerozoic regions, respectively. The shaded areas denote the CL inferred from surface wave tomography. The corresponding resolution matrices are displayed in panels d–f.

with thermal effects alone. Small values of ζ might signal compositional changes at larger depth, perhaps associated with the ocean-continent difference. Indeed, *AUS04-Vs* suggests very slow shear wave velocities between 100 and 200 km depth beneath the easternmost part of Australia, which appear continuous to the slow velocities observed beneath the oceanic domain at the east of Australia (Figure 1b). In contrast, variations in composition within the CL are required to explain the inferred scaling factors beneath the Proterozoic shield of central Australia. Purely thermal anomalies can explain $\zeta(r)$ for z $\leq$ 50 km, but the sharp decrease of ζ below this depth suggests that chemical depletion is present between 90 and 140 km depth. Similarly, chemical depletion seems to have occurred beneath the Archean province. We cannot propose a robust conclusion, however, because the tomographic model is poorly resolved and shows significant smearing in this region. An outstanding question is the nature and strength of chemical depletion. The scaling factor alone cannot resolve the trade-off between thermal and compositional effects. The amplitude of thermal and compositional variations can be inferred from appropriate statistical analysis of V_S and density distributions [*Deschamps and Trampert*, 2003], but independent information would be needed to constrain density better (e.g., the surface topography, provided it is correctly converted into dynamic topography) and the temperature (e.g., compressional-wave velocity model and heat flow data).

[15] The radial scaling factors that we infer are generally consistent with the tectosphere model due to *Jordan* [1988]. Beneath Precambrian terrains (here, restricted to the Proterozoic) the continental roots appear chemically distinct, whereas data for the Phanerozoic regions can be explained without significant compositional variations in the lithosphere. It is likely that the chemical depletion of the Proterozoic continental lithosphere contributes to the long term stability of the Australian continental roots, but from the work described in this paper it is yet not clear if chemical depletion by itself would be sufficient to prevent gravitational instability due to cooling. Rheology probably plays an important role [*Shapiro et al.*, 1999a; *Lenardic and Moresi*, 1999], but more systematic studies are necessary to understand the stability of a thermal boundary layer in a chemically depleted fluid.

References

Artemieva, I. M., and W. D. Mooney (2001), Thermal thickness and evolution of Precambrian lithosphere: A global study, *J. Geophys. Res.*, *106*, 16,387–16,414.

Bassin, C., G. Laske, and G. Masters (2000), The current limits of resolution for surface wave tomography in North America, *Eos Trans. AGU*, *81*(48), Fall Meet. Suppl., S12A-03.

Debayle, E., and B. L. N. Kennett (2000), The Australian continental upper mantle: Structure and deformation inferred from surface waves, *J. Geophys. Res.*, *105*, 25,423–25,450.

Debayle, E., and B. L. N. Kennett (2003), Surface-waves studies of the Australian region, *Spec. Publ. Geol. Soc. Aust.*, *22*, 25–45.

Deschamps, F., and J. Trampert (2003), Mantle tomography and its relation to temperature and composition, *Phys. Earth Planet. Inter.*, *140*, 277–291.

Deschamps, F., R. Snieder, and J. Trampert (2001), The relative density-to-shear velocity scaling in the uppermost mantle, *Phys. Earth Planet. Inter.*, *124*, 193–211.

Deschamps, F., J. Trampert, and R. Snieder (2002), Anomalies of temperature and iron in the uppermost mantle iferred from gravity data and tomographic models, *Phys. Earth Planet. Inter.*, *129*, 245–264.

Forte, A. M., and W. R. Peltier (1991), Viscous flow models of global geophysical observables: 1. Forward problems, *J. Geophys. Res.*, *96*, 20,131–20,159.

Forte, A. M., and H. C. Perry (2000), Geodynamic evidence for a chemically depleted continental tectosphere, *Science*, *290*, 1940–1944.

Forte, A. M., A. M. Dziewonsky, and R. J. O'Connell (1994), Thermal and chemical heterogeneity in the mantle: A seismic and geodynamic study of continental roots, *Phys. Earth Planet. Inter.*, *92*, 45–55.

Griffin, W. L., S. Y. O'Reilly, O. Gaul, and D. A. Ionov (1998), Secular variation in the composition of sub-continental lithospheric mantle: Geophysical and geodynamic implications, in *Structure and Evolution of the Australian Continent*, Geodyn. Ser., vol. 26, edited by J. Braun et al., pp. 1–26, AGU, Washington, D. C.

Jordan, T. H. (1978), Composition and development of the continental tectosphere, *Nature*, *274*, 544–548.

Jordan, T. H. (1988), Structure and formation of the continental tectosphere, *J. Petrol.*, Special Lithosphere Issue, 11–37.

Kogan, M. G., and M. K. McNutt (1993), Gravity field over northern Eurasia and variations in the strength of the upper mantle, *Science*, *259*, 473–479.

Lemoine, F. G., S. C. Kenyon, and J. K. Factor (1998), The Development of the Joint NASA GSFC and NIMA Geopotential Model EGM96, *NASA Tech. Pap., NASA/TP-1998–206861*, 575 pp.

Lenardic, A., and L.-N. Moresi (1999), Some thoughts on the stability of cratonic lithosphere: Effects of buoyancy and viscosity, *J. Geophys. Res.*, *104*, 12,747–12,758.

Mitrovica, J. X., and A. M. Forte (1997), Radial profile of the mantle viscosity: Results from the joint inversion of convection and postglacial rebound observables, *J. Geophys. Res.*, *102*, 2751–2769.

Pari, G., and W. R. Peltier (1996), The free-air gravity constraint on sub-continental mantle dynamics, *J. Geophys. Res.*, *101*, 28,105–28,132.

Perry, H. K. C., A. M. Forte, and D. W. S. Eaton (2003), Upper-mantle thermochemical structure below North America from seismic-geodynamic flow model, *Geophys. J. Int.*, *154*, 279–299.

Polet, J., and D. L. Anderson (1995), Depth extent of cratons as inferred from tomographic studies, *Geology*, *23*, 205–208.

Shapiro, S. S., B. H. Hager, and T. H. Jordan (1999a), Stability and dynamics of the continental tectosphere, *Lithos*, *48*, 115–133.

Shapiro, S. S., B. H. Hager, and T. H. Jordan (1999b), The continental tectosphere and Earth's long-wavelength gravity field, *Lithos*, *48*, 135–152.

Simons, F. J., A. Zielhuis, and R. D. van der Hilst (1999), The deep structure of the Australian continent from surface wave tomography, *Lithos*, *48*, 17–43.

Simons, F. J., R. D. van der Hilst, J.-P. Montagner, and A. Zielhuis (2002), Multimode Rayleigh wave inversion for heterogeneity and azimuthal anisotropy of the Australian upper mantle, *Geophys. J. Int.*, *151*, 738–754.

van der Hilst, R. D., B. L. N. Kennett, D. Christie, and J. Grant (1994), SKIPPY: Mobile broad-arrays to study the seismic structure of the lithosphere and mantle beneath Australia, *Eos Trans. AGU*, *75*, 177 and 180, 181.

Yoshizawa, K., and B. L. N. Kennett (2004), Multimode surface wave tomography for the Australian region using a three-stage approach incorporating finite frequency effects, *J. Geophys. Res.*, *109*, B02310, doi:10.1029/2002JB002254.

Zielhuis, A., and R. D. van der Hilst (1996), Upper-mantle shear velocity beneath eastern Australia from inversion of waveforms from SKIPPY portable arrays, *Geophys. J. Int.*, *127*, 1–16.

————————————

F. Deschamps and L. van Gerven, Department of Geophysics, Utrecht University, Budapestlaan 4, PO Box 80021, NL-3508 TA Utrecht, Netherlands. (deschamp@geo.uu.nl)

R. D. van der Hilst, Department of Earth, Atmospheric, and Planetary Sciences, Massachusetts Institute of Technology, Cambridge, MA 02139, USA.